Seasonal variations in arsenic mobility and bacterial diversity: The case study of Huangshui Creek, Shimen Realgar Mine, Hunan Province, China

Wenxu Li [a], Jing Liu [b,*], Karen A. Hudson-Edwards [c,*]

[a] The Key Laboratory of Solid Waste Treatment and Resource Recycle, Ministry of Education, Southwest University of Science and Technology, Mianyang 621010 China

[b] College of Resources and Environment, Southwest University, Chongqing 400716 China

[c] Environment & Sustainability Institute and Camborne School of Mines, University of Exeter, Penryn, Cornwall TR10 9DF, UK. Tel: +44(0)1326-259489.

Abstract

Rivers throughout the world have been contaminated by arsenic dispersed from mining activities. The biogeochemical cycling of this arsenic has been shown to be due to factors such as pH, Eh, ionic strength and microbial activity, but few studies have examined the effects of both seasonal changes and microbial community structure on arsenic speciation and flux in mining-affected river systems. To address this research gap, a study was carried out in Huangshui Creek, Hunan province, China, which has been severely impacted by long-term historic realgar (α-As_4S_4) mining. Water and sediment sampling, and batch experiments at different temperatures using creek sediment, were used to determine the form, source and mobility of arsenic. Pentavalent (AsO_4^{3-}) and trivalent arsenic (AsO_3^{3-}) were the dominant aqueous species (70-89 % and 30-11 %, respectively) in the creek, and the maximum concentration of inorganic arsenic in surface water was 10400 μg L^{-1}. Dry season aqueous arsenic concentrations were lower than those in the wet season samples. The sediments contained both arsenate and arsenite, and relative proportions of these varied with season. 8.3 tons arsenic per annum were estimated to be exported from Huangshui Creek. Arsenic release from sediment increased by 3 to 5 times in high water temperature batch experiments (25 and 37 °C)

* Corresponding author: (LIU JING) liujing-vip@163.com; (Karen A. Hudson-Edwards) k.hudson-edwards@exeter.ac.uk

compared to those carried out at low temperature (8 °C). Our data suggest that the arsenic-containing sediments were the main source of arsenic contamination in Huangshui Creek. Microbial community structured varied at the different sample sites along the creek. Redundancy analysis (RDA) showed that both temperature and arsenic concentrations were the main controlling factors on the structure of the microbial community. Protecbacteria, Bacteroidetes, Cyanobacteria, Firmicutes, Verrucomicrobia, and Planctomycetes were the stable dominant phyla in both dry and wet seasons. The genera *Flavobacterium*, *Hydrogenophaga* and *Sphingomonas* corrected with arsenic metabolism removal occurred in the most highly arsenic contaminated sites. Our findings indicate that seasonal variations profoundly control arsenic flux and species, microbial community structure and ultimately, the biogeochemical fate of arsenic.

Keywords: arsenic; seasonal variations; Huangshui Creek; fluxes; sediment; bacterial community

1. Introduction

Arsenic is highly toxic, and ingestion or inhalation of it can result in a wide range of carcinogenic, mutagenic and teratogenic health problems in humans (National Research Council, 1999). Arsenic (atomic number 33) belongs to Group V-A of the Periodic Table, closely resembling phosphorus chemically, and having common oxidation states of -III, 0, III, and V (Adriano 2001). Inorganic arsenite is more toxic and mobile than arsenate (Smedley and Kinniburgh, 2002). Both species are naturally present at high levels in the groundwater of a large number of countries (e.g., Bangladesh, India, Argentina, Hungary; Cullen and Reimer, 2010). Severe arsenic contamination has also been reported in mining areas around the world, including Cornwall (Camm et al., 2003), Yellowknife, Canada (Jamieson 2014), the Obuasi area of Ghana (Smedley et al., 1996), northern Chile (Smith et al., 1998), and the abandoned Songcheon Au-Ag mining area in Korea (Lee et al., 2008). In these areas, minerals such as arsenopyrite (FeAsS), arsenian pyrite ($Fe(AsS)_2$), realgar (α-As_4S_4) and orpiment (As_2S_3) are important sources of elevated concentrations of arsenic in mine wastes (Bowell et al., 1994; Craw and Pacheco, 2002; Lazareva et al., 2002). Arsenic-bearing mine wastes undergo microbially-influenced oxidative and reductive dissolution caused by flushing (Hering and Kneebone, 2002; Xie et al., 2014; Yu et al., 2014), resulting in the discharge of dissolved and colloidal arsenic to creek, river, lake and ground water. In these receiving bodies, the dominant aqueous species of arsenic are arsenite [AsO_3^{3-}] and arsenate [AsO_4^{3-}] (Plant et al., 2006). Matschullat (2000) and Zhu et al. (2014) respectively estimated that 4.3×10^3 to 7.3×10^4 tons of arsenic are discharged annually to the hydrosphere. However, the quantities, fluxes and speciation of arsenic in river systems are not well constrained.

Arsenic mobility in natural water is controlled by its speciation and environmental factors, such as pH, Eh, ionic strength and microbial activity. Arsenic speciation, in turn, can also vary due

to photooxidation, microbial Fe, Mn and As oxidation and reduction, and bacterial diversity (Ahmann et al., 1994; Mackay et al. 2014). For example, the Fe(III) in scorodite ($FeAsO_4 \cdot 2H_2O$) can be reduced to Fe(II) by the dissimilatory iron reducing bacterium *Shewanella alga BrY* (Cummings et al., 1999). This causes release of arsenic(V) from the scorodite, which is subsequently reduced to arsenic(III). Microbial reduction of arsenic(V) to arsenic(III) has also been shown to enhance arsenic mobilization from mine tailings (Macur et al., 2011).

Changes in biogeochemical factors related to seasonal conditions can also affect arsenic speciation and mobility (Sarmiento et al., 2007; Stuckey et al., 2015; Huang et al., 2018). These factors include available nutrients, micro-plankton abundance (Hasegawa, 1996), seasonal water temperature (Howard et al., 1995) and physical variation, such as ice cover (Palmer et al., 2019) and rainfall (Sultan, 2006). Eutrophication has also been shown to cause seasonal changes in arsenic speciation (Hasegawa et al., 2010; Yan et al., 2016). Seasonal changes also drive variations in climate, and profoundly affect organic mattter distribution, which further controls arsenic mobility in sediment (Galloway et al., 2018). For example, Galloway et al. (2018) and Palmer et al. (2019) investigated lake sediment which was affected by historic arsenopyrite-gold mining activity near Yellowknife, Northwest Territories, Canada. They showed that the distribution of arsenic in the sediment was related to both distance and direction from mine, and that anoxia and cryoconcentration were the main reasons for high arsenic concentrations in winter (Galloway et al., 2018; Palmer et al., 2019). Even though realgar (α-As_4S_4) is, like arsenopyrite (FeAsS), one of the common arsenic-hosting mineral in ore deposits, few studies have examined the effects of both seasonal changes and bacteria on arsenic speciation and flux in realgar mining-affected river systems.

Huangshui Creek drains the former Shimen Realgar Mine in Hunan Province, China, which

has the largest reserves of realgar in Asia, and operated for about 1500 years before closing in 2011 (Xiangyu et al., 2015, Tang et al., 2016). The former mining area is covered with large volumes of mine wastes containing arsenical fly ash and tailings. Runoff from these wastes flows into Huangshui Creek, potentially contaminating it with arsenic, and posing hazards to local residents in Huangchang residential areas and Heshan village that lie along the creek, and to the downstream Zaoshi Lake, which is the main water supply for Shimen County, Changde City. Therefore, Huangshui Creek is a typical case of a realgar mine waste-affected water course, and is thus an ideal study site for determining the effects of seasonal changes and microbes on arsenic mobility. This study aims to investigate the speciation and fate of arsenic in Huangshui Creek in dry and wet seasons, the indigenous bacterial communities, and the relationships between these. The results provide new understanding of the arsenic biogeochemical cycle in the study area, and also inform management of Huangshui Creek and other similarly affected river systems.

2. Materials and methods

2.1. Study site

Huangshui Creek is located in Hunan Province in the south of China (Fig. 1). It has a humid subtropical climate, with annual average temperature between 16 and 19 °C, and annual precipitation between 1200 and 1700 mm (Lu et al., 2015). The precipitation is uneven with respect to areal distribution and season, with a dry season between October and March and a wet season between April and September (Du et al., 2013; Lu et al., 2015). 69 % of annual precipitation occurs in the wet season due to the effects of monsoon circulation and topography (Li et al., 2000). Hunan Province is a mountainous region with complex topography.

Huangshui Creek is a tributary of the Xieshui River of the Li River Basin, one of the four

major rivers in Hunan. It rises in the mountains upstream of the Shimen Realgar Mine area, and flows from west to north-east across this area (Fig. 1). In the dry season, the creek is replenished by groundwater and surface water from the mountains. A hydrothermal spring occurs at site As4 (Fig. 1) along the creek. The Shimen Mine realgar and orpiment wastes (Fig. 1A) cover a total area of 1200 m^2 and are located on both sides of Huangshui Creek, approximately 30 m away from the channel. These wastes are transported to the tailings dam further downstream (Fig. 1). The creek flows through Huangchang residential areas (Fig. 1B) and Heshan Village to the tailings dam, dropping in elevation by approximately 50 m. Residential waste water and sewage are discharged directly into the creek through plastic pipes (Fig. 1C). A tailings dam (Fig. 1D) is situated close to the mountains, covering an area of about 150,000 m^2, and lying 20 m north of the creek. In this area, hot or normal springs from shallow hydrothermal deposit and crack flow into Huangshui Creek. The entire creek section from As1 to As9 has been channelized with concrete to dimensions of about 10 m wide and 1500 m long (Fig. 1C). Large amounts of mud are deposited in the low-flow portions of the creek in the Huangchang residential areas between As7 and As9.

2.2. Field methods

Water and sediments were sampled to evaluate seasonal changes in arsenic concentrations and species, and corresponding variations in bacterial communities. Sampling was performed in the dry and wet seasons (Du et al., 2013) over 2400 m of Huangshui Creek (29.65°~29.66°E, 111.03~111.04°N) (Fig. 1). Identical sampling processes were carried out in January 2018 (dry season) and August 2018 (wet season). Twelve surface water samples (As1 to As12; Fig. 1) were collected from 0.2-0.3 m below the water surface by combining two subsamples for each sample. Sample As4 was the site of the groundwater spring, sample As6 was a tributary and As11 was a hot

spring. Supplementary sampling of the sewage outflow near site As8 was carried out in July 2019. At each site, pH, Eh, and water temperature (T) were measured. Two groups of sediment samples were collected at same site from the top one cm at five sites in the creek (source of study area As1, groundwater inflow site As4, residential entrance site As7, residential exit site As9, end of study area As12). Five replicate samples were collected from the top 1 cm of sediment by stainless scraper and sediment sampler at each of the five sampling locations (As1, As4, As7, As9, and As12), for a total of 25 samples, for bacteria 16S rRNA gene amplicon sequencing. The second group for the above five sites was collected for geochemical analysis and dynamic batch dissolution experiments. These samples were dried at 60 °C, and the replicates were combined to make a composite sample, which was then sieved to less than 100 mesh (<150 μm). Water and sediment samples were stored storage in portable frozen and liquid nitrogen boxes, respectively. Arsenic speciation and bacteria sequence analyses were completed within in one week of sampling.

. *2.3. Aqueous sample collection analysis*

pH, Eh and water temperature were determined in the field using a portable HACH composite Eh-pH-T meter. At each site, two sub-samples were mixed to form a composite sample and filtered using 0.22 μm cellulose membranes. The concentration of total arsenic (arsenic(T)) was determined using inductively coupled plasma emission spectrometer (ICP-AES, iCPA6500 Thermo Fisher) with a detection limited of 0.1 μg L^{-1}.

The quantification and specification of aqueous arsenic was determined using hydride generation-atomic fluorescence spectrometry coupled with high-performance liquid chromatography (HPLC-AFS, Jitian, China). The procedures are described fully in Fan et al. (2017, 2018). Arsenic acid ($C(AsO_4^{3-})$=0.233 ± 0.005 μ mol g^{-1}) and arsenicus acid ($C(AsO_3^{3-})$=1.011 ± 0.016 μmol g^{-1}) (National Sharing Platform for Reference Materials, National Institute of Metrology,

China) were used to derive the calibration curves for HPLC-LAS analysis. Total arsenic was quantified using ICP-AES. The precision difference in the result of total arsenic between the HPLC-AFS and ICP-AES analysis was ± 5%. Larger deviations (> ± 5%) among seasonal samples were observed when measuring the creek water samples. These differences may have been due to other species of arsenic that were not identified by HPLC-AFS. However, for the purposes of this study we neglected the <1 % organic arsenic that was determined. In the HPLC-AFS analysis, we observed a strong arsenate peak and a very weak arsenite peak after a 1000 times dilution. As a result, we attributed the difference between total arsenic from HPLC-AFS and arsenate from ICP-AES to arsenite, as we did in our other studies (e.g., Jimei et al., 2018). No homologous differences were observed in lab arsenic release experiments.

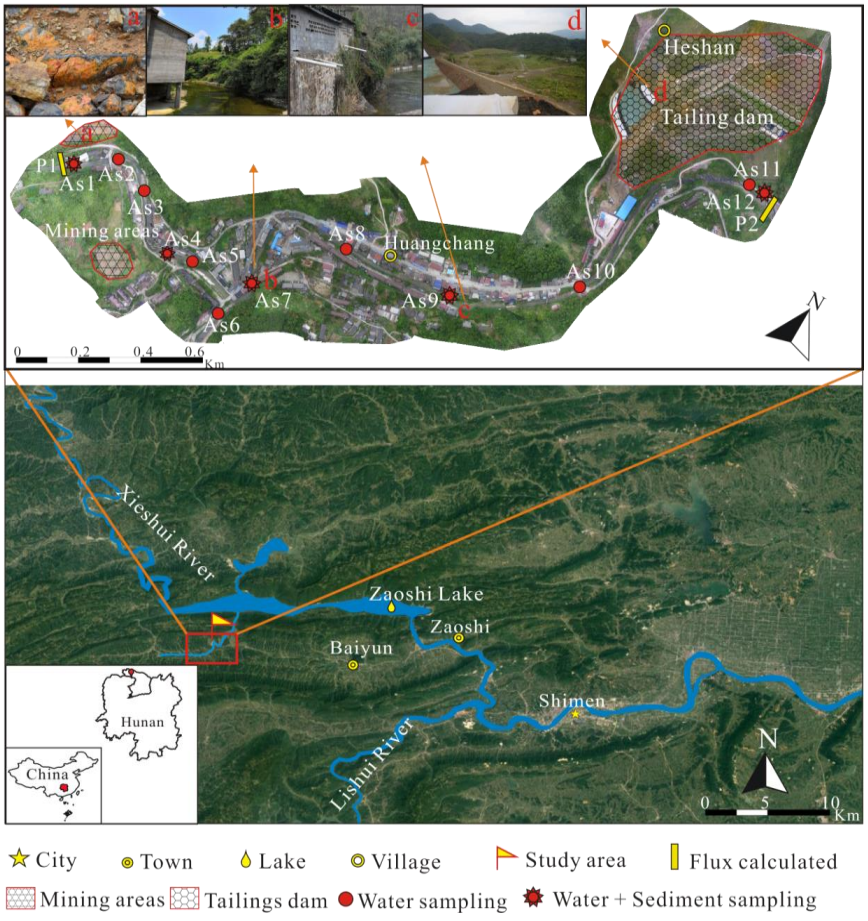

Fig.1. Location of the study area and sampling sites.

2.4. Mineralogical characteristics of sediments

The major oxide compositions of the wet sediment samples were determined using X-ray fluorescence (XRF; PANalytical Axios instrument) equipped with a rhodium anode. After pre-digestion 3 h with nitric acid at 100 °C, the wet and dry season sediment samples were digested in a solution of nitric, hydrochloric, and hydrofluoric acids (5:3:2, v/v/v) in a microwave. Total arsenic concentrations were subsequently determined by ICP-AES (iCAP-6500, ThermoFisher). Light irradiation on the sediments was examined by Fourier Transform Infrared spectrometry (FTIR, Spectrum, Perkin Elmer) coupled with a diamond attenuated total reflection (ATR). Spectra ranging from 400~4000 cm^{-1} were obtained with 64 scans per sample with a resolution of 1 cm^{-1} and a mirror velocity of 0.6329 cm s^{-1}.

Mineralogical analysis was carried out by X-ray diffraction (XRD) using a PANalyticalX'Pert PRO X-ray diffractometer with Cu-Kα radiation. The operating conditions were 15 kV, 40 mA, 2θ from 10° to 80°, and scan and time step increments of 0.03° and 10.16 s, respectively. For micromorphological analysis, sediment samples were dried and impregnated with epoxy resin under vacuum. A section of about 1 cm was then cut, polished, mounted on a glass slide, and ground and polished to ca. 20 μm thickness. These thin sections were observed under petrological polarizing microscopy (Wild M21, Wild Heerbrugg Ltd.). Surface morphologies of the sediment samples were observed using Scanning Electron Microscopy (SEM, EVO@18, ZEISS) with energy-dispersive-X-ray -spectroscopy (EDX) operating at 15 kV. X-ray Photoelectron spectroscopy (XPS) was used to characterize arsenic speciation in the sediment samples. XPS was conducted with a monochromatized Al-Kα source at 30 eV and a step size of 0.05 eV (XPS, R3000, VG-Scienta).

2.5. Dynamic arsenic dissolution

Batch experiments were performed to analyze the magnitude of, and effect of temperature on, potential arsenic release from the sediment samples. In this experiment, all five composite wet season sediment samples were subjected to the same procedures. A rotary shaker (150 rpm) was used and set to temperatures of 8, 25 and 37 °C. In order to ensure that the reaction temperature of the experiment was correct at the outset of the experiments, the 25 mL empty serum bottles and 100 mL deionized water were shaken for 24 h in corresponding temperature before each experiment. Solution pH values were adjusted to 7.0 by adding hydrochloric acid or sodium hydroxide. Subsequently, 20 mL of this solution and 0.1 g sediment were added to the serum bottle. For each site, duplicate analyses were carried out. One mL aliquots were sampled from the suspensions at 2, 6, 12, 24, 36 and 48 h, and were passed through 0.22 μm cellulose membrane filters for arsenic analysis by HPLC-AFS.

2.6. Flux calculation

The bankfull width and depth of each site were measured by matering band after simplifying five equidistant blocks. The area of cross section (S_{sum}) at each site was determined as the sum of all block area (S_i, i=1, 2…n, n≤3), which equaled the produce of the specific depth of block (D_i, m) and the width (W_i, m). The instantaneous velocity (V_i, m/s) at each block was measured by a Doppler ultrasonic sensor PVM portable flowmeter (Sigma, America). The flux of arsenic (F_{As}) was obtained by the following equation:

$$F_{As}=\sum_i^n C_{As(T)} \times S_i^n \times V_i^n$$

where F_{As} is the arsenic flux of the flow section (μg s^{-1}) and $C_{As(T)}$ is the total arsenic

concentrations in surface water (μg L^{-1}). The arsenic flux from all sites was measured for balance verification, and the export quantity of arsenic toward downstream lake, which is attributed to the mine area, equals the difference between A1 and A12 (Fig. 1).

2.7. DNA extraction and purification of sediments

The genome DNA from the sediment samples was extracted using the CTAB/SDS method (Niu et al., 2008). The DNA concentration and purity was monitored on 1% agarose gels, and then was diluted to 1 ng μL^{-1} with distilled water.

2.8. High-throughput bacteria 16S rRNA gene amplicon quenching and analysis of sediments

The genes of the diluted DNA were amplified using 515F and 806R primers to target the V4 regions of the bacterial 16S rRNA genes. All PCR reactions were carried out with Phusion® High-Fidelity PCR Master Mix (New England Biolabs). Subsequently, the same volume of the SYB green-containing buffer with PCR products and operate electrophoresis on 2% agarose gels detection. The PCR products were mixed in equal density ratios and purified using a GeneJETTM Gel Extraction Kit (Thermo Scientific). Sequencing libraries were generated using the NEB Next® Ultra ™ DNA Library Prep Kit for Illumia (NEB, USA). The data analysis was based on the Raw PE, which was obtained from an Illumia MiSeq platform. For each site, the five composite samples were used to extract the DNA and allow the sequence data to be incorporated a group. The single-end reads were assigned to samples based on their unique barcode and truncated by cutting off the barcode and primer sequence. Quality filtering on the raw reads was performed under specific filtering conditions to obtain the high-quality clean reads according to the Cutadapt (Martin, 2011) (V1.9.1, http://cutadapt.readthedocs.io/en/stable/) quality controlled process. Further details

of the quenching and analysis are summarised in Table S1.

All of the sequence files for the dry and wet season samples are available from the NCBI GenBank with the accession numbers PRJNA493908 (SUB4579024) and PRJNA511650 (SUB4969544).

3. Results and discussion

3.1 Quantification and speciation of arsenic and effects of seasonal variability

Huangshui Creek is an important source of water for domestic activity in Heshan village and Huangchang residential areas, and it discharges into Zaoshi Lake (Fig. 1). In the dry season, the pH was neutral to alkaline (7.45~8.54) (Table S2). The pH of most sites became higher in wet season, ranging from 7.66 to 10.61. This may have been due to more intense water-rock interaction between the creek water and the underlying calcite-bearing bedrock in the wet season. Compared to the other sites, As7, As8 and As9 have higher pH (10.21~10.61) and lower Eh values (-181.67~-204.10 mV), suggesting that human activities and habitation around these sites may have impacted on the redox and pH of the Huangshui Creek (Table S2). The use of detergents and eutrophication in the residential areas may have caused the increased alkalinity (Chang, 2008). Concentrations of aqueous arsenic(T), arsenic(III) and arsenic(V) during the dry and wet seasons are shown in Fig. 2A and 2B, respectively. Arsenic(T) concentrations in surface water were 280-10400 and 30-8980 μg L^{-1} in the dry and wet seasons, respectively, and annual arsenic(T) averages were 155-9700 μg L^{-1}. Increases and decreases in aqueous arsenic(V) concentrations followed those of aqueous arsenic(T). The average total aqueous arsenic concentration in the dry season (3953 μg L^{-1}) was not statistically different to that in the wet season and (4005 μg L^{-1}). Aqueous arsenic(V) concentrations exceeded those of arsenic(III) in the wet season, but the reverse was true in the dry season (Figure 2). This

contrasts with previous work in Huangshui Creek, which showed that the main aqueous arsenic species was As(V) (Wang et al., 2015). Wet season concentrations and percentages of aqueous arsenic(III) were greater in the dry season (15%-93%) than in the wet season (10%-15%), but this was not reflected in the Eh measurements. This may have been due to inaccurate measurements or bacterial activity. The highest aqueous arsenic concentrations occurred downstream of the mining areas and the groundwater spring (As1-As4). The tributary (As6) provided virtually no aqueous arsenic to Huangshui Creek. The hydrothermal and normal springs at As4 and As11, respectively, provided ca. 2000 μg L^{-1} of aqueous arsenic(T) in both the wet and dry seasons, and the sewage outflow contributed 2380 μg L^{-1} of aqueous As(T).

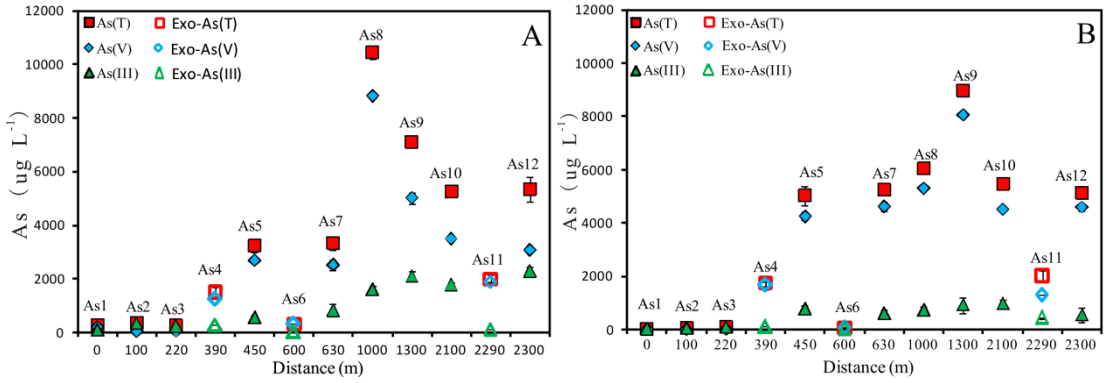

Fig. 2. Variations in aqueous arsenic concentrations in dry (A) and wet (B) seasons. As(T): total inorganic arsenic; arsenic(V): pentavalent arsenic; arsenic(III): trivalent arsenic; exo-: exogenous arsenic (As4, groundwater spring; As6, tributary; As11, spring).

3.2. Geochemical and mineralogical characteristics of sediments

XRF geochemical data for the dry season sediments are summarized in Table S4. The samples were enriched in SiO_2 (52.27-70.61 wt. %), Al_2O_3 (15.14-17.56 wt. %), CaO (2.60-17.10 wt. %), Fe_2O_3 (5.30-6.82 wt. %), K_2O (2.94-3.79 wt. %), MgO (1.44-2.07 wt. %), TiO_2 (0.69-0.85 wt. %), and P_2O_5 (0.87-1.45 wt. %).). Significant differences in arsenic concentrations were observed in each site As1 (dry 120 μg g^{-1}; wet 103 μg g^{-1}), As4 (dry 590 μg g^{-1}; wet 521 μg g^{-1}), As7 (dry 964

μg g^{-1}; wet 1310 μg g^{-1}), As9 (dry 992 μg g^{-1}; wet 1700 μg g^{-1}); As12 (dry 564 μg g^{-1}; wet 675 μg g^{-1}). Concentrations of arsenic in samples As7 and As9 were the highest, and are comparable to those in other mining-affected river sediments (Azcue et al. 1994, Leon et al. 2018). Wet season arsenic concentrations in samples As7, As9 and As12 were higher than their respective dry season concentrations.

No arsenic-containing minerals were found by XRD analysis. Analysis of sediment under the polarizing microscope showed that the sediment contains clay, altered hematite, sandstone and biological debris (Fig. 4, S2). SEM-EDX analysis of the most arsenic-enriched sample (As9) suggested that the arsenic is associated with Fe and Si-O, which may represent an arsenic-bearing Fe oxyhydroxide coating on quartz (Fig. 4). The presence of Al and K in As9 confirmed the presence of clay minerals (observed with the polarizing microscope), and these appear to have had arsenic-bearing Fe oxide coatings. Such arsenic-bearing Fe oxides are found commonly in mine wastes (e.g., Walker et al., 2005; Kossoff et al., 2012).

The XPS As 2P 3/2 spectrum for sample As9 is presented in Fig. S3. There is a very weak peak in the As_{2p} range, suggesting that the sample may contain both pentavalent (1326.80 eV) (Wagner 1975) and trivalent arsenic (1322.70 eV) (Taylor 1982).

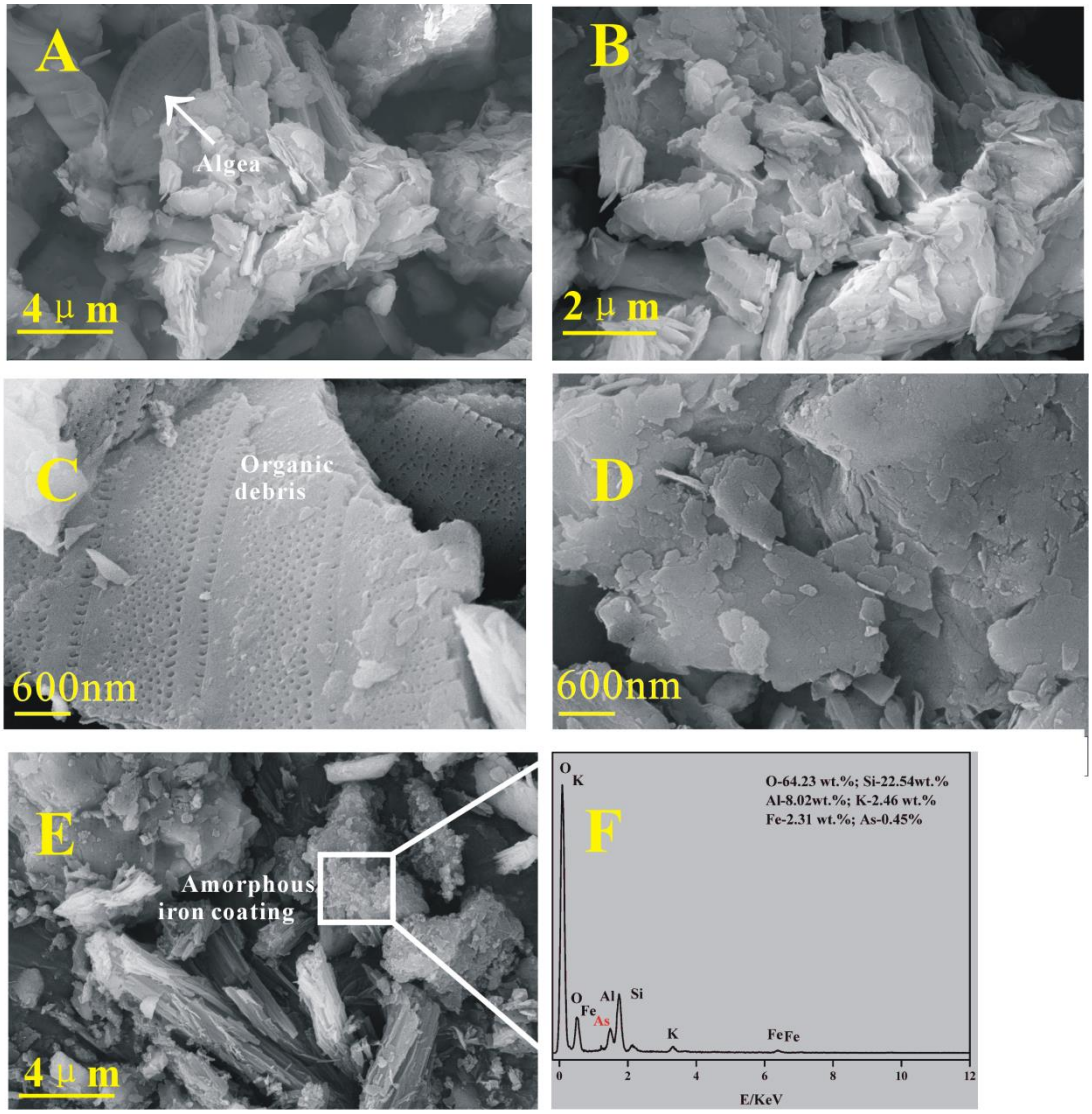

Fig.4. SEM images of sediment samples As1(a), As4(b), As7(c), As12(d), As9(e), and the EDX spectra for As9(f).

The ATR-FTIR spectra of the dry and wet season sediments from Huangshui Creek are shown in Fig. 5A and 5B, respectively. The main vibration and assignments for arsenic and sulfur are shown in Table S3. The broad peaks at 1004 and 1003 cm^{-1} were assigned to v_3 vibrations of SO_4^{2-} (Usher et al., 2004, Roonasi and Holmgren, 2009), and vibrations for both AsO_4^{3-} and AsO_3^{3-} were also observed. In the dry season, the only obvious vibrations in sample As1 occurred at 796 and 772 cm^{-1}, and these were assigned to the v_1 vibration of AsO_3^{3-}. Such v_1 AsO_3^{3-} vibrations have been observed in aqueous $As(OH)_3$ (Goldberg and Johnston, 2001) and in tooeleite

($Fe_6(AsO_3)_4SO_4(OH)_4 \cdot 4H_2O$) (Liu et al., 2013). The intensity of these two peaks gradually increased downstream from As1 to As7 and then decreased in As9, similar to the pattern of the arsenic(III) concentrations in water samples collected in the dry season. A peak of weak intensity was observed in 872 cm^{-1} for sample As7 and As9, and this was attributed to the v_3 vibration of AsO_4^{3-} (Liu et al., 2017). This confers with the aqueous species analysis, which showed that AsO_4^{3-} concentrations in samples As7 and As9 were higher than those in the other samples.

The FTIR spectra for the wet season sediment samples displayed obvious characteristic peaks (Fig. 3B). The peaks at 910 cm^{-1} (Goldberg and Johnston 2001), 872 and 463 cm^{-1} (Liu et al. 2017) that were attributed to AsO_4^{3-} were observed in all wet season samples, but not in the dry season samples. The intensity of peaks from SO_4^{2-} (1003 cm^{-1}), AsO_4^{3-} (910, 872 and 463 cm^{-1}) and AsO_3^{3-} vibrations (796 and 772 cm^{-1}) gradually increased downstream from As1 to As9 and decreased in As12, following the trends of aqueous AsO_4^{3-} and AsO_3^{3-} concentrations in the wet season.

Two broad and weak peaks were observed at 1636 cm^{-1} and 1415 cm^{-1} in the spectrum for sample As9 only. These were attributed to water bending and nitrate vibrations (Sánchez et al., 2008), respectively. Site As9 was located downstream of the Huangchang residential areas, and was likely affected by residential wastewater discharge and urban drainage.

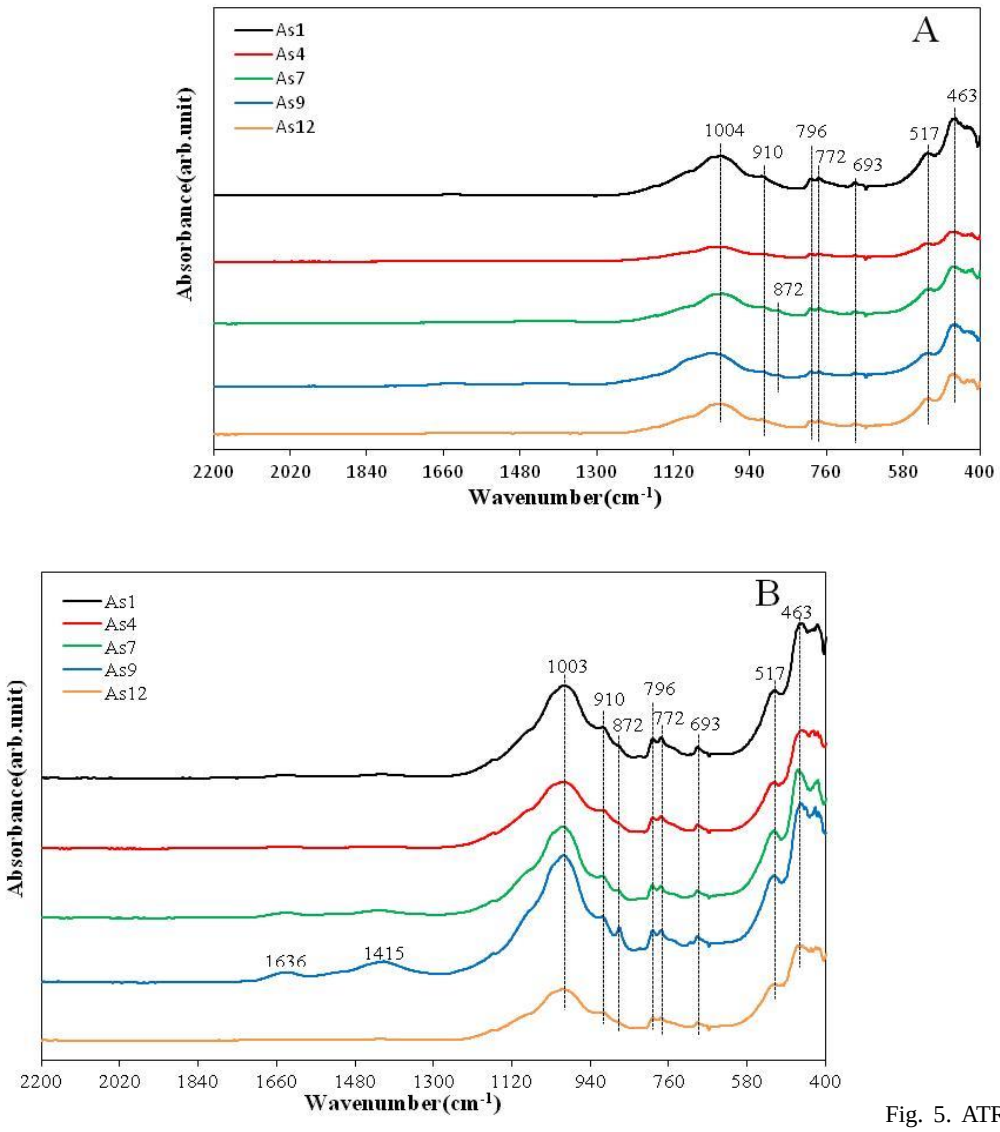

Fig. 5. ATR-FTIR spectra of sediment samples in the dry season (A) and wet season (B).

3.3. Sources of arsenic to Huangshui Creek

Our water and sediment data suggest that possible sources of arsenic to Huangshui Creek waters include the realgar mine, creek sediments, hydrothermal and hot springs, urban runoff and sewage discharge (Fig. 2). Aqueous arsenic concentrations were highest in the residential areas (from 450 m downstream throughout the study area). Some of this arsenic was probably sourced from the hydrothermal and normal springs (As4 and As11) and the sewage outflow (near As9), both of which have concentrations around 2000 μg L^{-1} arsenic(T). Aqueous arsenic(T) concentrations in

samples As5 to As10 and As12 were higher than this value, suggesting contributions from other sources. Runoff from the realgar mine wastes in the upper part of the study area was likely one of these sources, since concentrations were highest downstream, and lowest upstream, of these wastes (Fig. 2). Arsenic(T) concentrations peaked between 700 to 1000 m downstream of the mine waste areas, however, suggesting that there was another source. Given the relatively high arsenic(T) concentrations in the sediments at this location (As7 and As9; Table S5), the source may have been the large amounts of mud here (Chi et al., 2017). This hypothesis is explored further in the dynamic laboratory release experiments discussed in section 3.5.

3.4 Fluxes of arsenic in Huangshui Creek

Fluxes of creek water and arsenic(T), determined by the field tests, are shown in Fig. 6. Fluxes of both were low at the beginning of the monitored area, but increased significantly at the end. The calculated fluxes of arsenic(T) from beginning to end were 15600 and 30100 g d^{-1} in the dry and wet seasons, respectively. The calculated annual total arsenic(T) flux was ca. 8.3 tons.

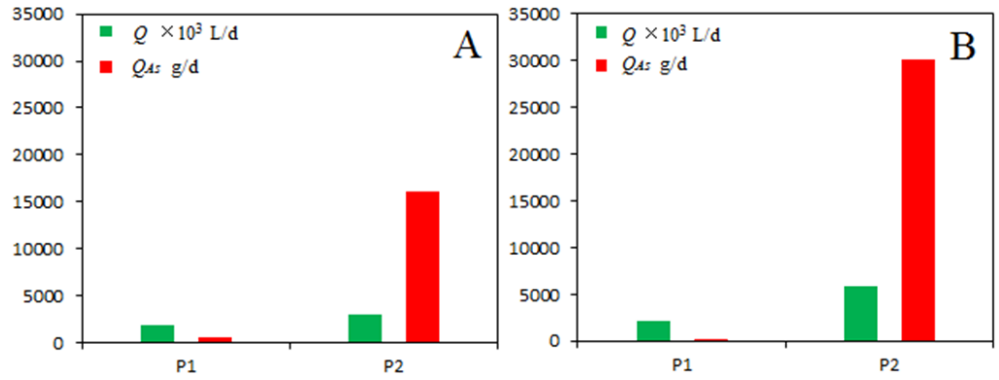

Fig. 6. Flux of creek water and total arsenic in dry (A) (P1: the beginning of the monitored section) and wet (B) seasons (P2: the end of the monitored section). Q represents discharge of creek per day, 10^3 L^{-1} d (Green); Q_{As} represents discharge of arsenic mass per day, g d^{-1} (Red).

3.5. Dynamic release of arsenic from sediments and possible environmental effects

Leachate concentrations of arsenic(V) and arsenic(III) determined in the 8, 25 and 37 ℃ batch experiments are shown in Fig. 5. The concentrations varied with site location and temperature. In the 8 ℃ experiments, sample As7 released the highest amounts of arsenic(V) and arsenic(III) after 48 hours (up to 333 μg L^{-1} and 139 μg L^{-1}), followed by As9 (<0.1 and 360 μg L^{-1}), As4 (95 and 135 μg L^{-1}), As12 (<0.1 and 135 μg L^{-1}) and As1 (<0.1 μg L^{-1}). The released arsenic concentrations of samples As7 and As9 were higher than those of the other samples, possibly because sites As7 and As9 were located in the slow flowing region downstream of the realgar mine and because they had higher arsenic(T) concentrations than the other samples (Table S5). Total arsenic release was 2.93 to 3.46 times higher in all samples when the experimental temperature was increased to 25 ℃. Arsenic(V) and arsenic(III) concentrations increased to 378 and 1380 μg L^{-1} at 37 ℃ for As7. These results suggest that increasing temperature resulted in increased arsenic (especially arsenic(III)) release from the sediment. Over the first 12 h of the 25 and 37 ℃ experiments, the extent of arsenic(V) and arsenic(III) release gradually increased in all samples, except for site As1, for which no As was released. As the experiment progressed, dissolved arsenic(V) concentrations decreased and arsenic(III) dramatically increased in samples As7 and As9.

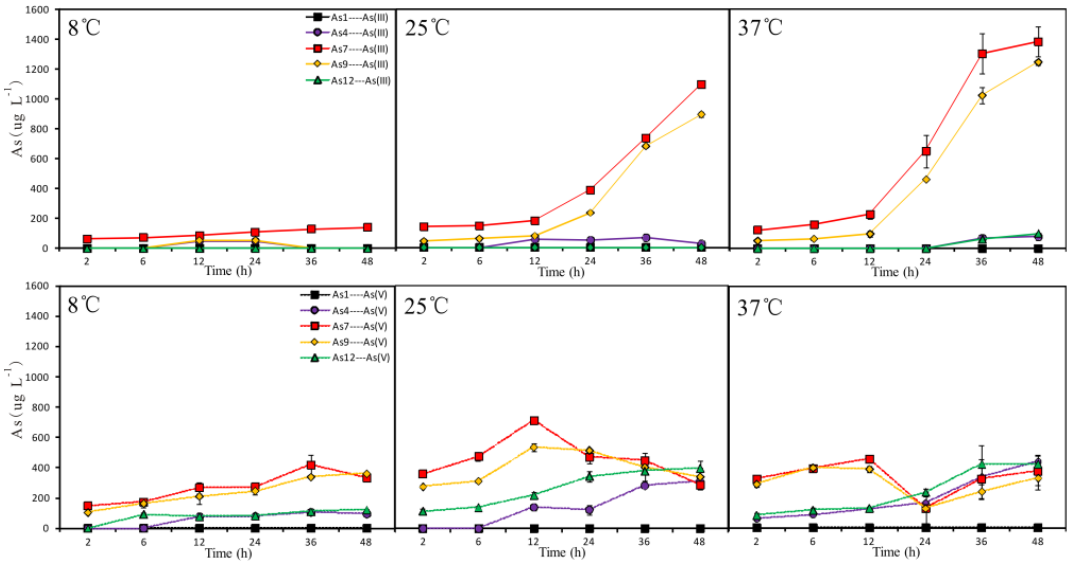

Fig. 5. Changes of arsenic concentration in different temperature experiment (8°, 25° and 37°C).

3.6. Microbial species evenness, richness and diversity

The Illumina-based analysis of the V4 region of the 16S rRNA genes for Bacteria amplicons yielded 2,130,965 raw reads, with 1,995,697 clean reads after splicing and quality control, from all 25 dry season samples. The sequence of 16S rRNA produced 2,068,247 raw reads, and 1,995,303 clean reads, from the 25 wet season samples. 16S rRNA genes were amplified successfully from all dry and wet season samples. All sequences with ≧97% similarity were assigned to the same OTUs. 9410 and 8196 different OTUs were generated for the dry and wet seasons, respectively. One hundred and eighteen (1.25%) and 67 (0.81%) different OTUs were assigned to Archaea in the dry and wet season samples, respectively. These results were on the same order of magnitude as those for Zn-, Pb- and Cu-contaminated riparian soils, in which the 0.58% OTUs were assigned to Archeae (Fan et al. 2016). The dry season OTUs mapped to 58 phyla, 147 classes, 181 orders, 330 families, 598 genera and 311 species, whereas 55phyla, 131 classes, 193 orders, 348 families, 784 genera, 457 species were mapped in the wet season samples. Rarefaction curves for the dry (Fig. S4A) and wet (Fig. S4B) season sediments indicated that the sequencing had good sample depth.

Alpha indices for diversity estimation are shown in Table 2. The coverage estimation revealed that more than 98% of species were recovered, which suggests that the sequence data are representative of the true bacterial community. Richness estimates and diversity indices were higher in the dry season samples. This may be due to the higher concentrations of arsenic in the wet season sediment samples, as high concentrations of As have been shown to reduce the bacterial diversity (Lorenz et al. 2006, Leon et al. 2018). The α-diversity of Shannon, Chao and ACE were lowest in samples As7 and As9, consistent with the sediment dissolution experiments, which showed that samples As7 and As9 released the most arsenic at all temperatures.

Table 2. Diversity estimation of 16Sr RNA

Season	Group	Observed species	Coverage (%)	Diversity index		Richness estimator	
				Shannon	Simpson	Chao1	ACE
Dry	As1	3728	98.3	9.813	0.996	4159.455	4233.775
	As4	3397	98.3	9.608	0.995	3834.463	3900.214
	As7	2256	98.8	8.351	0.989	2616.546	2668.896
	As9	1745	99.0	7.811	0.987	2034.069	2110.815
	As12	3102	98.5	9.533	0.995	3471.988	3546.870
Wet	As1	2317	99.3	8.601	0.991	2546.731	2548.607
	As4	2622	99.3	8.132	0.971	2833.225	2852.819
	As7	1976	99.3	7.541	0.964	2189.885	2229.723
	As9	2174	99.2	8.295	0.984	2438.102	2495.421
	As12	2706	99.1	8.741	0.991	3033.860	3078.729

3.6. Bacterial compositions, community structures and their response to the seasonal variation

The bacteria community structures of the dry and set season sediment sites at the phylum level are shown in Fig. 8. Proteobacteria (dry season relative abundance 35.63~54.25 %; wet season relative abundance 42.85~68.75%), Bacteroidetes (dry 14.65~41.41 %; wet 8.17~12.17 %), Cyanobacteria (dry 1.37~14.27 %; wet 1.81~12.42 %), Firmicutes (dry 0.57~5.00 %; wet 2.04~11.78 %), Verrucomicrobia (dry 2.83~7.70 %; wet 1.65~3.83 %), and Planctomycetes (dry

0.58~5.99 %; wet 1.73~4.89 %) represented the most top six dominate phylum in the dry and wet season samples. Nitrospirae (0.25~4.96 %), Acidobacteria (0.12~4.14 %), Spirochaetes (0.05~1.98 %), and Parcubacteria (0.27~2.65 %) were additional dominate phyla in the dry season. Chloroflexi (0.46~2.93 %), Actinobacteria (0.96~2.83 %), Saccharibacteria (0.49~1.22 %), Deinococcus Thernus (0.19~1.05 %) represented the least abundant phyla in wet season. Proteobacteria, Bacteroidetes, Bacteroidetes, and Verrucomicrobia have been shown to be abundant in metal-contaminated sediments (Tomczyk-Żak et al. 2013, Fan et al. 2016, Leon et al. 2018). There were significant differences in the bacterial communities between each site in the dry and wet seasons. At sites As7 and As9 the sequences affiliated with the most dominant six phyla comprised more than 90% of the total classified bacterial sequences in both the dry and wet season sediments. Cyanobacteria, traditionally assigned to algae (Brandes et al., 2016) or hydrophyte (Kenyon et al., 1972, Ishida and Al, 1997), were unexpectedly abundant in Huangshui Creek, indicating the existence of algae or aquatic plants (cf., Arash et al., 2016). Ulla et al. (2012) found that Cyanobacteria produced potently toxic microcystins that could threaten ecosystems, so these may also have affected the Huangshui Creek microorganisms. The diversity of Proteobacteria in each sample was much richer in the arsenic-rich wet season samples; this may have been due to the tolerance of Proteobacteria to arsenic contamination. The ten most abundant genera for each sampling site differed between wet and dry seasons, except for an unidentified Chloroplast (Table S6). *Flavobacterium* (relative abundance, 1.67~17%), *Arcicella* (0.02~0.34%), an unidentified Chloroplast (0.85~13.34%), *Phormidium* (0.02~2.33%), *Arenimonas* (3.34~6.96%), *Arcobacter* (0.01~2.49%), *Polymorphobacter* (0.12~2.12%), *Hydrogenophaga* (0.28~4.57%), unidentified *Nitrospiraceae* (0.25~4.87%) were the dominate genera in the dry season samples. *Haematospirillum* (0.01~6.46%), *Phyllobacterium* (0.17~11.35%), *Sphingomonas* (0.14~4.82%),

Brevundimonas (0.05~3.72%), *Roseomonas* (0.56~4.21%), *Dechloromonas* (0.22~6.58%), *Nannocystis* (0.03~3.25%), *an* unidentified *Chloroplast* (0.88~10.22%), *Faecalibacterium* (0.09~3.30%) and *Bacteroides* (0.11~1.53%). The unidentified *Chloroplast*, the mutual dominate genera, was also reported as the most abundant genera in arsenic-, cadmium-, lead- and zinc-contaminated soil (Zeng et al., 2019), and Katharina et al. (2007) pointed out it can promote biofilm development.

Seasonal variations in bacterial abundances have been attributed to several factors. Katharina et al. (2007) suggested that flow velocity was the main physical factor affecting the incongruency of bacterial community structures, and Crump and Hobbie (2005) suggested that seasonal community changes may be due to variations in climate, temperature and stream geochemistry. In the dry season, the abundances of *Flavobacterium* and *Hydrogenophaga* genera significantly increased in the high arsenic sites (As7 and As9), in accordance with previous studies (Fan et al. 2010, Li et al. 2013, Lian et al. 2014, Joung et al. 2016, Sun et al. 2016). *Flavobacterium* genera are arsenic-resistant and can methylate arsenic (Honschopp et al., 1996; Jenkins et al., 2002) and *Hydrogenophaga* genera are arsenite oxidisers (vanden Hoven and Santini, 2004). In the wet season samples, *Nannocystis* was significantly ($P<0.01$) abundant at sites As7 and As9, and its presence may have been due to wastewater bioflocculants (cf., Zhang et al., 2002). *Sphingomonas* has been shown to be abundant in metal-contaminated soil samples (Wang et al., 2018) and to efficiently reduce arsenic(V) (Wang and Zhao, 2009).

The relative contribution of geochemical factors in Huangshui Creek water to microbial composition and community were expressed by redundancy analysis (RDA) plots in Fig. 9. RDA analysis showed that total arsenic (As(T)), pH and temperature (T) of the water had an equal influence on the microbial communities. In the dry season, the microbial communities in sites As9

As12 were affected more intensely by the arsenic concentration variation than others, and site As7 was affected more by the pH variation. No obvious interdependency was observed between microbial communities and temperature in the dry season. We propose that this was mainly due to the lower temperature in the dry season. In the wet season, the microbial communities in sites As7, As9 and As12 were severely affected by arsenic concentration, pH and temperature. The similarities of microbial communities in these downstream sites suggests a more stable biocenosis. These findings are similar to those of Riina et al. (2004), Lorenza et al. (2006), Al Lawati et al. (2012) and Sheik et al. (2012), who showed that microbial communities were influenced by distribution of arsenic, and that the total arsenic in overlying water correlated with high arsenic sediment sites. The latter observation may imply that the arsenic in overlying water was released from the sediment by physicochemical dissolve, microbiophagy or other mechanisms, which is consistent with our results. Furthermore, it can be seen from the RDA plots that concentrations of total arsenic positively correlated with pH, which may be attributed to mineral dissolution (Burlo et al., 1999; Yamaguchi et al., 2011), and temperature, as demonstrated by the batch experiments.

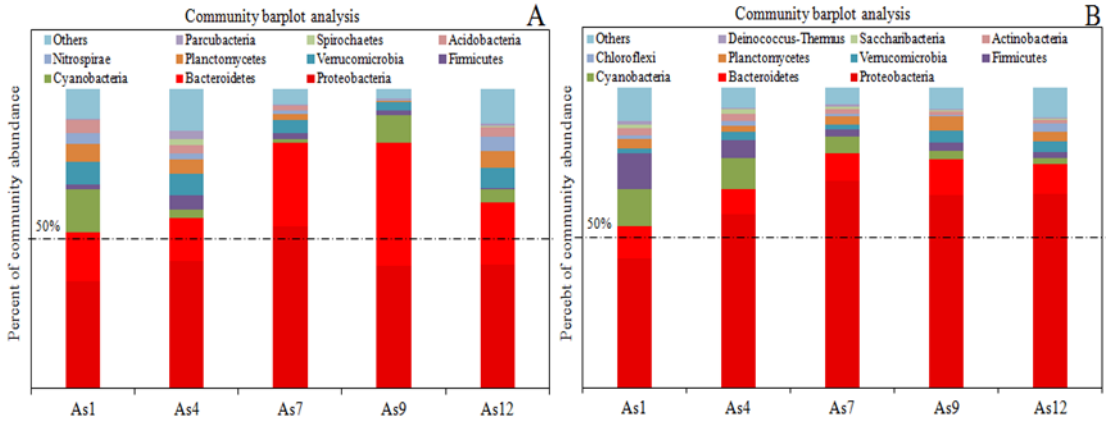

Fig. 8. Relative abundance of bacterial top ten phyla in dry (A) and wet (B) seasons.

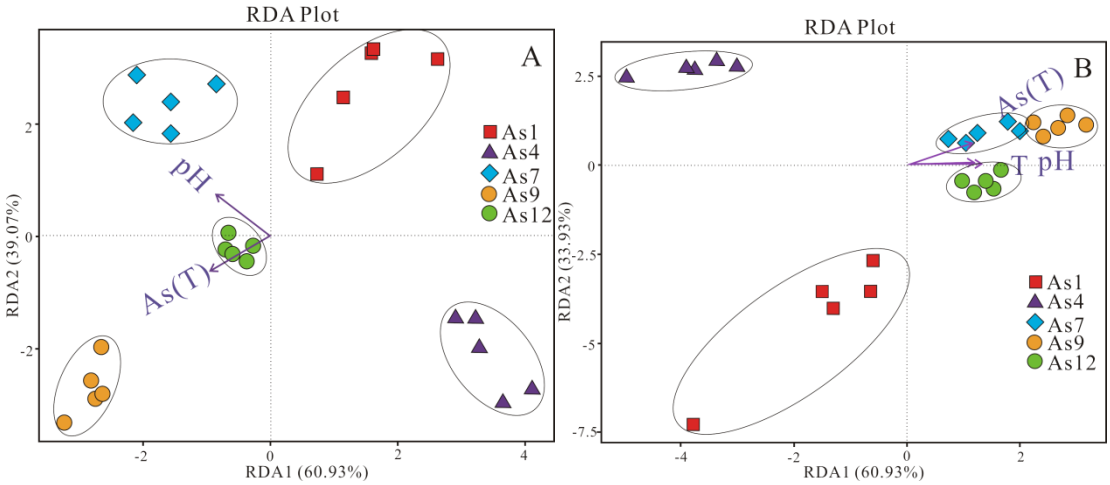

Fig.9. RDA plots analysis of genus and geochemical factors in overlying water at five sediment sites. A: RDA analysis in dry season; B: RDA analysis in wet season; pH; As: total arsenic; T: temperature.

3.7. Possible mechanisms of release of arsenic to Huangshui Creek

As summarized above, possible sources of arsenic to Huangshui Creek waters include the realgar mine wastes, creek sediments, hydrothermal and hot springs and sewage discharge (Fig. 2). Arsenic(V) was directly discharged to the creek from the springs and sewage discharge (Figs. 1c, 2). Both arsenic(III) and arsenic(V) occurred throughout the creek. The FTIR data, SEM results and dynamic sediment arsenic release experiments (Figs. 3, 4 and 5) suggest that these species could have been released from arsenic-bearing Fe oxides in the sediments, but it is also possible that they could have been derived from realgar weathering in the mine wastes. The microbial analysis showed that high levels of arsenic contamination limited bacterial diversity, but allowed for enrichment of microbes able to oxidise arsenic(III) and reduce arsenic(V). This suggests that microbes were likely involved in the cycling of arsenic in Huangshui Creek. Seasonal variations in water and sediment-borne arsenic concentrations and speciation were likely due to temperature variations (as suggested by the dynamic sediment release experimental results) and to more intense sediment-water interactions in the wet season (Fig. 5). Based on the batch experiment results for

As7, it is suggested that sediment-water interactions released 1400 μ g L^{-1} arsenic(III) at 37℃, 167 μ g L^{-1} arsenic(III) at 8℃ and ca. 360 μ g L^{-1} arsenic(V). Redox variations could have also caused seasonal variations in arsenic concentrations, although this was not determined by the batch experiments. Such seasonal redox changes may in turn have been due to localized anoxia in the dry season (preserving arsenic(III)) or to differences in microbial activity.

The laboratory dissolution experiments provided evidence that the arsenic-contaminated creek sediments could be a major source of arsenic contamination in the creek. Based on the dynamic dissolution experiments, hydrological parameters and bacteria community analysis, we propose a schematic model arsenic released in Huangshui Creek (Fig. 10). The genera *Flavobacterium*, *Hydrogenophaga* and *Sphingomonas* are correlated with oxidation, reduction or methylation of arsenic. The model in Figure 10 also suggests that adsorption/precipitation processes and microbial and hydrophyte activity were responsible for arsenic cycling in Huangshui Creek.

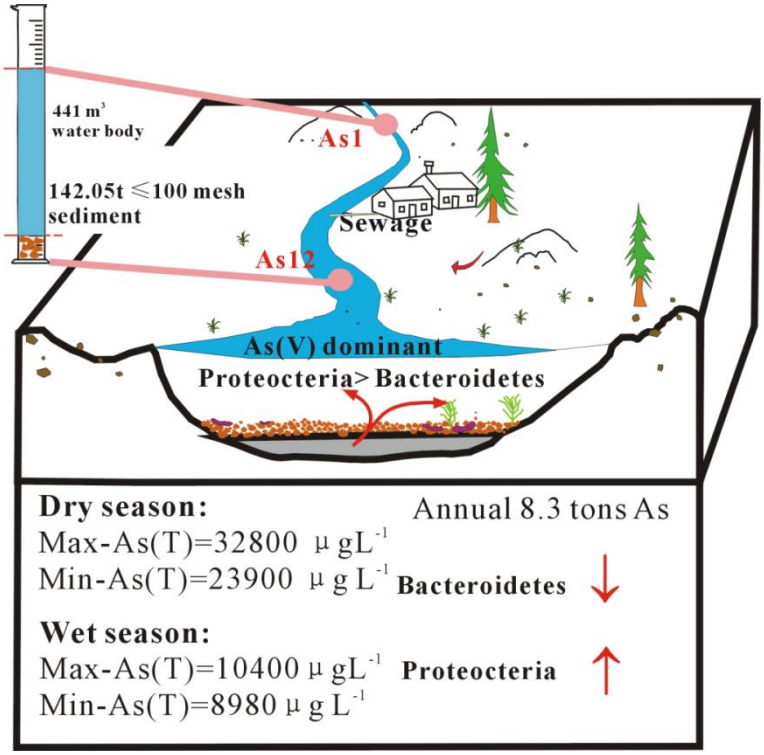

Fig. 10. Schematic presentation of release arsenic from sediments in Huangshui Creek and its corresponding water/solid model

4. Potential environmental risk

High-quality realgar extracted from the Shimen Mine (Fig. 11A) was used as a raw material in the glass and firecracker industries. Due to long-term exposure to arsenic-containing dust, water and crops, several miners and local residents have suffered severe skin disease (Fig. 11B). For these reasons, the original intake water supply for the village was completely supplanted in 2014 by a centralized and unified water supply system. Hyperaccumulation plants (eg. *Pteris vittata L.*) have been planted in Huangshui Creek to extract arsenic from soil. However, significant accumulation of arsenic has occurred, and probably still occurs, in Zaoshi Lake. Therefore, the related environmental risks need to be evaluated further. Although we propose that sediment from of Huanghui Creek is the main source for aqueous arsenic, we have not evaluated the potential contribution of leaching of the mine waste dam or its nearby soil. Desilting of the creek is strongly advised to reduce the severity of this arsenic source. According to our results, the risk of arsenic contamination of surface water is higher in the summer season compared to the winter season.

Fig. 11. Realgar product of high purity from Yanfeng Chemical Company, Changsha City, Hunan province (>93%) from Shimen mine (1990s) (A) and skin disease of local residents (B).

5. Conclusions

This study investigated the aqueous geochemical and microbial variations in arsenic-containing Huangshui Creek, which has been affected by historical realgar mining in Hunan Province, China. Our major findings are summarized as follows:

a) Huangshui Creek is seriously contaminated by inorganic arsenic, with maximum aqueous concentrations up to 10400 μg L^{-1}. Arsenate was the main arsenic species (70 % to 89 %), and the creek water was alkaline and weak reducing. There were notable variations in total aqueous arsenic concentrations in wet and dry seasons.

b) Sediments from the creek displayed characteristic arsenate and arsenite ATR-FTIR peaks that varied with season. Sediments collected downstream of the realgar mine were the most arsenic-enriched (454~1060 μg g^{-1}).

c) Batch experiments using Huangshui Creek sediments showed that high water temperatures (25 and 37 ℃) significantly increased arsenic release (by 3-5 times).

d) Release of arsenic from creek bottom sediments may have been major sources of arsenic to Huangshui Creek. Arsenic mobility was controlled by absorption/precipitation to sediment and by microbial and hydrophyte activity.

e) Protecbacteria, Bacteroidetes, Cyanobacteria, Firmicutes, Verrucomicrobia, and Planctomycetes were the stable dominate phyla in dry and wet season sediments. Seasonal change resulted in fluctuations in the abundance of Protecbacteria and Bacteroidetes, which could have affected arsenic speciation. *Flavobacterium*, *Hydrogenophaga* and *Sphingomonas* genera corrected with arsenic metabolism removal occurred in the most highly arsenic contaminated sites. Arsenic contamination, temperature and pH in both water and sediment influenced the bacterial community.

Acknowledgements

The authors would like to thank Jianwen He for sampling assistance. This study was supported by the National Natural Science Foundation of China (Grant No. 41772367).

Appendix A. Supplementary data

Supplementary data to this article can be found online at XXXX.

References

Adriano, D.C., 2001. Arsenic. Trace Elements in Terrestrial Environments: Biogeochemistry, Bioavailability, and Risks of Metals. New York, NY, Springer New York: 219-261.

Ahmann, D., Roberts, A.L., Krumholz, L.R., Morel, F.M., 1994. Microbe grows by reducing arsenic. Nature 371, 750.

Al Lawati, W.M., Rizoulis, A., Eiche, E., Boothman, C., Polya, D.A., Lloyd, J.R., Berg, M. Vasquez-Aguilar, P., van Dongen, B.E., 2012. Characterisation of organic matter and microbial communities in contrasting arsenic-rich Holocene and arsenic-poor Pleistocene aquifers, Red River Delta, Vietnam. Appl. Geochem. 27, 315-325.

Azcue, J.M., Mudroch, A., Rosa, F., Hall, G.E.M., 1994. Effects of abandoned gold mine tailings on the arsenic concentrations in water and sediments of Jack of Clubs Lake, B.C. Environ. Technol. Lett. 15, 669-678.

Barringer, J.L., Reilly, P.A., Eberl, D.D., Blum, A.E., Bonin, J.L., Rosman, R., Hirst, B., Alebus, M., Cenno, K., Gorska, M., 2011. Arsenic in sediments, groundwater, and streamwater of a glauconitic Coastal Plain terrain, New Jersey, USA—Chemical “fingerprints” for geogenic and

anthropogenic sources. Appl. Geochem. 26, 763-776.

Benson, B.J., J. D. Lenters, J.D., dagger, Magnuson, J.J., Stubbs, M., Kratz, T.K., Dillon, P.J., Hecky, R.E., Lathrop, R.C. 2010. Regional coherence of climatic and lake thermal variables of four lake districts in the Upper Great Lake Region of North America. Freshwater Biol. 43, 517-527.

Bhowmick, S., Nath, B., Halder, D., Biswas, A., Majumder, S., Mondal, P., Chakraborty, S., Nriagu, J., Bhattacharya, P., Iglesias, M., 2013. Arsenic mobilization in the aquifers of three physiographic settings of West Bengal, India: Understanding geogenic and anthropogenic influences. J. Hazard. Mater. 262, 915-923.

Bissen, M., Frimmel, F.H., 2003. Arsenic—a review. Part I: occurrence, toxicity, speciation, mobility. Acta Hydrochim. Hydrobiol. 31, 9-18.

Bowell, R.J., Morley, N.H., Din, V.K., 1994. Arsenic speciation in soil porewaters from the Ashanti Mine, Ghana. Appl. Geochem. 9, 15-22.

Brandes, J., Kuhajek, J.M., Goodwin, E., Wood, S.A., 2016. Molecular characterisation and co-cultivation of bacterial biofilm communities associated with the mat-forming diatom Didymosphenia geminata. Microb. Ecol. 72, 514-525.

Burlo, F., Carbonell-Barrchina, A., Jugsujinda, A., Anurakpongsatorn, P., Delaune, R.D., Sirisukhodom, S., 1999. The influence of redox chemistry and pH on chemically active forms of arsenic in sewage sludge-amended soil. Environ. Int. 25, 613-618.

Byrd, J.T., 1988. The seasonal cycle of arsenic in estuarine and nearshore waters of the South Atlantic Bight. Mar. Chem. 25, 383-394.

Camm, G.S., Butcher, A.R., Pirrie, D., Hughes, P.K., Glass, H.J., 2003. Secondary mineral phases associated with a historic arsenic calciner identified using automated scanning electron

microscopy; a pilot study from Cornwall, UK. Miner. Eng. 16, 1269-1277.

Chi, S., Hu, Zheng, J., Dong, F., 2017. Study on the effects of arsenic pollution on the communities of macro-invertebrate in Xieshui River. Acta Ecol. Sin. 37, 1-9.

Craw, D., Pacheco, L., 2002. Mobilisation and bioavailability of arsenic around mesothermal gold deposits in a semiarid environment, Otago, New Zealand. Sci. World J. 2, 308-319.

Crump, B.C., Hobbie, J.E., 2005. Synchrony and seasonality in bacterioplankton communities of two temperate rivers. Limnol. Oceanogr. 50, 1718-1729.

Cullen, W.R., Reimer, K.J. 2010. Arsenic speciation in the environment. Chem. Rev. 89, 713-764.

Cummings, D.E., Caccavo, F., Fendorf, S., Rosenzweig, R.F., 1999. Arsenic mobilization by the dissimilatory Fe (III)-reducing bacterium Shewanella alga BrY. Environ. Sci. Technol. 33, 723-729.

Chang, H., 2008. Spatial analysis of water quality trends in the Han River basin, South Korea. Water Res. 42, 3285-3304.

Du, J., Fang, J., Xu, W., Shi, P., 2013. Analysis of dry/wet conditions using the standardized precipitation index and its potential usefulness for drought/flood monitoring in Hunan Province, China. Stoch. Environ. Res. Risk Assess. 27, 377-387.

Deng, Y., Li, H.,Wang, Y., Duan, Y., Gan, Y., 2014. Temporal variability of groundwater chemistry and relationship with water-table fluctuation in the Jianghan Plain, Central China. Proc. Earth Planet. Sci. 10, 100-103.

Du, J., Fang, J., Xu, W., Shi, P., 2013. Analysis of dry/wet conditions using the standardized precipitation index and its potential usefulness for drought/flood monitoring in Hunan Province, China. Stoch. Environ. Res. Risk Assess. 27, 377-387.

Fan, H., Su, C.W., Yao, J., Zhao, K., Wang, Y., Wang, G., 2010. Sedimentary arsenite-oxidizing and

arsenate-reducing bacteria associated with high arsenic groundwater from Shanyin, Northwestern China. J. Appl. Microbiol. 105, 529-539.

Fan, L., Zhao, F., Jing, L., Hudson-Edwards, K.A., 2018. Dissolution of realgar by Acidithiobacillus ferrooxidans in the presence and absence of zerovalent iron: Implications for remediation of iron-deficient realgar tailings. Chemosphere 209, 381-391.

Fan, L., Zhao, F., Liu, J., Frost, R.L., 2017. The As behavior of natural arsenical-containing colloidal ferric oxyhydroxide reacted with sulfate reducing bacteria. Chem. Eng. J. 332, 183-191.

Fan, M., Lin, Y., Huo, H., Liu, Y., Zhao, L., Wang, E., Chen, W., Wei, G., 2016. Microbial communities in riparian soils of a settling pond for mine drainage treatment. Water Res. 96, 198-207.

Galloway, J. M., Swindles, G. T., Jamieson, H. E., Palmer, M., Parsons, M. B., Sanei, H., Macumber, A. L., Patterson, R. T., Falck, H. 2018. Organic matter control on the distribution of arsenic in lake sediments impacted by ~65 years of gold ore processing in subarctic Canada. Sci. Total Environ. 622-623, 1668-1679.

Goldberg, S., Johnston, C.T., 2001. Mechanisms of arsenic adsorption on amorphous oxides evaluated using macroscopic measurements, vibrational spectroscopy, and surface complexation modeling. J. Colloid Interf. Sci. 234, 204-216.

Hering, J.G., Kneebone, P.E., 2002. Biogeochemical controls on arsenic occurrence and mobility in water supplies. Environmental Chemistry of Arsenic, W.T. Frankenberger (Ed.), Marcel Dekker, New York, Basel, pp. 155-181.

Hasegawa, H., 1996. Seasonal changes in methylarsenic sistribution in Tosa Bay and Uranouchi Inlet. Appl. Organomet. Chem. 10, 733-740.

Hasegawa, H., Rahman, M. A., Kitahara, K., Itaya, Y., Maki, T., Ueda, K., 2010. Seasonal changes

of arsenic speciation in lake waters in relation to eutrophication. Sci. Total Environ. 408, 1684-1690.

Howard, A. G., Comber, S. D. W., Kifle, D., Antai, E. E., Purdie, D. A., 1995. Arsenic speciation and seasonal changes in nutrient availability and micro-plankton abundance in Southampton Water, U.K. Estuar. Coast. Shelf Sci. 40, 435-450.

Huang, K., Liu, Y., Yang, C., Duan, Y., Yang, X., Liu, C., 2018. Identification of hydrobiogeochemical processes controlling seasonal variations in arsenic concentrations within a riverbank aquifer at Jianghan Plain, China. Water Res. Res. 54, 4294-4308.

Honschopp, S., Brunken, N., Nehrkorn, A., Breunig, H. J., 1996. Isolation and characterization of a new arsenic methylating bacterium from soil. Microbiol. Res. 151, 37-41.

Ishida, T., Al, E., 1997. Phylogenetic relationships of filamentous cyanobacterial taxa inferred from 16S rRNA sequence divergence. J. Gen. Appl. Microbiol 43, 237-241.

Jamieson, H.E., 2014. The legacy of arsenic contamination from mining and processing refractory gold ore at Giant Mine, Yellowknife, Northwest Territories, Canada. Rev. Mineral. Geochem. 79, 533-551.

Jimei, Z., Shu, C., Jing, L., Frost, R.L., 2018. Adsorption kinetic and species variation of arsenic for As(V) removal by biologically mackinawite (FeS). Chem. Eng. J. 354, 237-244.

Joung, Y., Kang, Kim, H., Kim, T.S., Han, J.H., Kim, B.S., Ahn, T.S., Joh, K., 2016. Flavobacterium paronense sp. nov., isolated from freshwater of an artificial vegetated island. Int. J. Syst. Evol. Microbiol. 66, 365-370.

Kenyon, C.N., Rippka, R., Stanier, R.Y., 1972. Fatty acid composition and physiological properties of some filamentous blue-green algae. Arch. Mikrobiol. 83, 216-236.

Kling, G.W., Kipphut, G.W., Miller, M.M., O'Brien, W.J., 2010. Integration of lakes and streams in

a landscape perspective: the importance of material processing on spatial patterns and temporal coherence. Freshwater Biol. 43, 477-497.

Kossoff, D., Hudson-Edwards, K.A., Dubbin, W.E., Alfredsson, M., Geraki, T., 2012. Cycling of As, Pb, Pb and Sb during weatheirng of mine tailings: implications for fluvial environments. Miner. Mag. 76, 1209-1228.

Lazareva, E.V., Shuvaeva, O.V., Tsimbalist, V.G., 2002. Arsenic speciation in the tailings impoundment of a gold recovery plant in Siberia. Geochem. Explor. Environ. Anal. 2, 263-268.

Lee, J.S., Lee, S.W., Chon, H.T., Kim, K.W., 2008. Evaluation of human exposure to arsenic due to rice ingestion in the vicinity of abandoned Myungbong Au–Ag mine site, Korea. J. Geochem. Explor. 96, 231-235.

Lu, J., Zeng, M., Zeng, X., Fang, Z., Yuan, J., 2015. Analysis of ice-covering characteristics of China Hunan Power Grid. IEEE Trans. Ind. Appl. 51, 1997-2002.

Li, J. B., Zheng, Y. Y., Gao, C. H., Yang, Y., 2000. A discussion on geographical regularity of flood and drought in Hunan Province. J. Nat. Disasters 9, 115-120.

Leon, C.G., Moraga, R., Valenzuela, C., Gugliandolo, C., Lo, G.A., Papale, M., Vilo, C., Dong, Q., Smith, C.T., Rossello-Mora, R., 2018. Effect of the natural arsenic gradient on the diversity and arsenic resistance of bacterial communities of the sediments of Camarones River (Atacama Desert, Chile). Plos One 13, e0195080.

Li, P., Wang, Y., Jiang, Z., Jiang, H., Li, B., Dong, H., Wang, Y., 2013. Microbial diversity in high arsenic groundwater in Hetao Basin of Inner Mongolia, China. Geomicrobiol. J. 30, 897-909.

Lian, A., Xian-Chun, Z., Yao, N., Yao, M., Lingli, Z., Xuesong, L., 2014. Flavobacterium arsenatis sp. nov., a novel arsenic-resistant bacterium from high-arsenic sediment. Int. J. Syst. Evol. Microbiol. 64, 3369-3374.

Liu, J.-L., Yao, J., Wang, F., Min, N., Gu, J.-H., Li, Z.-F., Sunahara, G., Duran, R., Solevic-Knudsen, T., Hudson-Edwards, K.A., Alakangas, L., 2019. Bacterial diversity in typical abandoned multi-contaminated nonferrous metal(loid) tailings during natural attenuation. Environ. Pollut. 247, 98-107.

Liu, J., Cheng, H., Frost, R.L., Dong, F., 2013. The mineral tooeleite $Fe_6(AsO_3)_4SO_4(OH)_4 \cdot 4H_2O$ – An infrared and Raman spectroscopic study-environmental implications for arsenic remediation. Spectrochim. Acta A Mol. Biomol. Spectrosc. 103, 272-275.

Liu, J., He, L., Dong, F.Q., Frost, R.L., 2017. Infrared and Raman spectroscopic characterizations on new Fe sulphoarsenate hilarionite ($Fe_2((III))(SO_4)(AsO_4)(OH) \cdot 6H_2O$): Implications for arsenic mineralogy in supergene environment of mine area. Spectrochim. Acta Pt. A Mol. Biomol. Spectrosc. 170, 9-13.

Lorenz, N., Hintemann, T., Kramarewa, T., Katayama, A., Yasuta, T., Marschner, P., Kandeler, E., 2006. Response of microbial activity and microbial community composition in soils to long-term arsenic and cadmium exposure. Soil Biol. Biochem. 38, 1430-1437.

Mackay, A. A., Gan, P., Yu, R., Smets, B.F., 2014. Seasonal arsenic accumulation in stream sediments at a groundwater discharge zone. Environ. Sci. Technol. 48, 920-929.

Macur, R.E., Wheeler, J.T., McDermott, T.R., Inskeep, W.P., 2001. Microbial populations associated with the reduction and enhanced mobilization of arsenic in mine tailings. Environ. Sci. Technol. 35, 3676-3682.

Magnuson, J.J., Benson, B.J., Kratz, T.K., 2010. Temporal coherence in the limnology of a suite of lakes in Wisconsin, U.S.A. Freshwater Biol. 23, 145-159.

Martin, M., 2011. Cutadapt removes adapter sequences from high-throughput sequencing reads. EMBnet.journal 17, 10-12.

Matschullat, J., 2000. Arsenic in the geosphere—a review. Sci. Total Environ. 249, 297-312.

Ma, J.Z., Wang, X.S., Edmunds, W.M., 2005. The characteristics of ground-water resources and their changes under the impacts of human activity in the arid Northwest China—a case study of the Shiyang River Basin. J. Arid Environ. 61, 277-295.

Nadakavukaren, J.J., Ingermann, R.L., Jeddeloh, G., Falkowski, S.J., 1984. Seasonal variation of arsenic concentration in well water in Lane County, Oregon. Bulletin of Environ. Contam. Toxicol. 33, 264-269.

National Research Council, 1999. Arsenic in Drinking Water, National Academic Press, Washington, D.C.

Niu, C., Kebede, H., Auld, D.L., Woodward, J.E., Burow, G., Wright, R.J., 2008. A safe inexpensive method to isolate high quality plant and fungal DNA in an open laboratory environment. Afr. J. Biotechnol. 7, 2818-2822.

Olías, M., Nieto, J.M., Sarmiento, A.M., Cerón, J.C., Cánovas, C.R., 2004. Seasonal water quality variations in a river affected by acid mine drainage: the Odiel River (South West Spain). Sci. Total Environ. 333, 267-281.

Palmer, M. J., Chételat, J., Richardson, M, Jamieson, H. E., Galloway, J. M., 2019. Seasonal variation of arsenic and antimony in surface waters of small subarctic lakes impacted by legacy mining pollution near Yellowknife, NT, Canada. Sci. Total Environ. 684, 326-339.

Plant, J.A., Kinniburgh, D.G., Smedley, P.L., Fordyce, F.M., Klinck, B.A., 2006. Arsenic and selenium. Treatise Geochem. 9, 17-66.

Rice, K.C., Conko, K.M., Hornberger, G.M., 2002. Anthropogenic sources of arsenic and copper to sediments in a suburban lake, Northern Virginia. Environ. Sci. Technol. 36, 4962-4967.

Riina, T., Timo, K., Häggblom, M.M., 2004. Microbial community structure and activity in arsenic-,

chromium- and copper-contaminated soils. Fems Microbiol. Ecol. 47, 39-50.

Roonasi, P., Holmgren, A., 2009. An ATR-FTIR study of sulphate sorption on magnetite; rate of adsorption, surface speciation, and effect of calcium ions. J. Colloid Interf. Sci. 333, 27-32.

Sánchez, M. T., Pérez-Pariente, J., Márquez-Alvarez, C., 2008. Dynamics of PEO-PPO-PEO block copolymer aggregation and silicate mesophase formation monitored by time-resolved ATR-FTIR spectroscopy. Stud. Surf. Sci. Catal. 174, 333-336.

Sarmiento, A.M., Oliveira, V., Gómez-Ariza, J.L., Nieto, J.M., Sánchez-Rodas, D., 2007. Diel cycles of arsenic speciation due to photooxidation in acid mine drainage from the Iberian Pyrite Belt (Sw Spain). Chemosphere 66, 677-683.

Savarimuthu, X., Hira-Smith, M.M., Yuan, Y., Ehrenstein, O.S.V., Das, S., Ghosh, N., Mazumder, D.N.G., Smith, A.H., 2006. Seasonal variation of arsenic concentrations in tubewells in West Bengal, India. J. Health Popul. Nutr. 24, 277-281.

Sheik, C.S., Mitchell, T.W., Rizvi, F.Z., Rehman, Y., Faisal, M., Hasnain, S., Mcinerney, M.J., Krumholz, L.R., 2012. Exposure of soil microbial communities to chromium and arsenic alters their diversity and structure. Plos One 7, e40059.

Smedley, P., Edmunds, W., Pelig-Ba, K., 1996. Mobility of arsenic in groundwater in the Obuasi gold-mining area of Ghana: some implications for human health. Geol. Soc. London Spec. Publ. 113, 163-181.

Smith, A.H., Goycolea, M., Haque, R., Biggs, M.L., 1998. Marked increase in bladder and lung cancer mortality in a region of Northern Chile due to arsenic in drinking water. Am. J. Epidemiol. 147, 660-669.

Stuckey, J.W., Schaefer, M.V., Benner, S.G., Fendorf, S., 2015. Reactivity and speciation of mineral-associated arsenic in seasonal and permanent wetlands of the Mekong Delta. Geochim.

Cosmochim. Acta 171, 143-155.

Sultan, K., Dowling, K., 2006. Seasonal changes in arsenic concentrations and hydrogeochemistry of Canadian Creek, Ballarat (Victoria, Australia). Water Air Soil Pollut. 169, 355-374.

Sun, J. Q., Xu, L., Liu, M., Wang, X.Y., Wu, X.L., 2016. Flavobacterium suaedae sp. nov., an endophyte isolated from root of Suaeda corniculata. Int. J. Syst. Evol. Microbiol. 66, 1943-1949.

Tang, J., Liao, Y., Yang, Z., Chai, L., Yang, W., 2016. Characterization of arsenic serious-contaminated soils from Shimen realgar mine area, the Asian largest realgar deposit in China. J. Soils Sed. 16, 1519-1528.

Taylor, J. A., 1982. An XPS study of the oxidation of AlAs thin films grown by MBE. J. Vac. Sci. Technol. 20, 751-755.

Tomczyk-Żak, K., Kaczanowski, S., Drewniak, Ł., Dmoch, Ł., Sklodowska, A., Zielenkiewicz, U., 2013. Bacteria diversity and arsenic mobilization in rock biofilm from an ancient gold and arsenic mine. Sci. Total Environ. 461-462, 330-340.

Ulla, K., Fewer, D.P., Jouni, J., Matti, W., Kaarina, S., Jouko, R., 2012. Cyanobacteria produce a high variety of hepatotoxic peptides in lichen symbiosis. PNAS 109, 5886-5891.

Usher, C.R., Cleveland, C.A., Strongin, D.R., Schoonen, M.A., 2004. Origin of oxygen in sulfate during pyrite oxidation with water and dissolved oxygen: An in situ horizontal attenuated total reflectance infrared spectroscopy isotope study. Environ. Sci. Technol. 38, 5604-5606.

Vanden Hoven, R.N., Santini, J.M., 2004. Arsenite oxidation by the heterotroph Hydrogenophaga sp. str. NT-14: the arsenite oxidase and its physiological electron acceptor. Biochimica et Biophysica Acta (BBA) – Bioenergetics. 1656, 148-155.

Wagner, C.D., 1975. Chemical shifts of Auger lines, and the Auger parameter. Faraday Discuss. Chem. Soc. 60, 291-300.

Walker, S.R., Jamieson, H.E., Lanzirotti, A., Andrade, C.F., Hall, G.E.M., 2005. The speciation of arsenic in iron oxides in mine wastes from the Giant Gold mine, N.W.T.: Application of synchrotron micro-XRD and micro-XANEs at the grain scale. Can. Mineral. 43, 1205-1224.

Wang, S., Zhao, X., 2009. On the potential of biological treatment for arsenic contaminated soils and groundwater. J. Environ. Manage. 90, 2367-2376.

Wang, T., Yuan, Z., Yao, J., 2018. A combined approach to evaluate activity and structure of soil microbial community in long-term heavy metals contaminated soils. Environ. Eng. Res. 23, 62-69.

Xiangyu, Z., Rucheng, W., Xiancai, L., 2015. Secondary minerals of weathered orpiment-realgar-bearing tailings in Shimen carbonate-type realgar mine, Changde, Central China. Mineral. Petrol. 109, 1-15.

Xie, X., Wang, Y., Li, J., Wu, Y., Duan, M., 2014. Soil geochemistry and groundwater contamination in an arsenic-affected area of the Datong Basin, China. Environ. Earth Sci. 71, 3455-3464.

Wang, X., Hu, Y., Zhou, L., L, X., Xu, F., Wand, L., Mo, D., Zhou, L., 2015. Arsenic contamination in Shimen Realgar Mine I：As spatial distribution, chemical fractionations and leaching. JAES 34,1515-1521.

Yamaguchi, N., Nakamura, T., Dong, D., Takahashi, Y., Amachi, S., Makino, T., 2011. Arsenic release from flooded paddy soils is influenced by speciation, Eh, pH, and iron dissolution. Chemosphere 83, 925-932.

Yu, Q., Wang, Y., Ma, R., Su, C., Wu, Y., Li, J., 2014. Monitoring and modeling the effects of groundwater flow on arsenic transport in Datong Basin. J. Earth Sci. 25, 386-396.

Yan, C., Che, F., Zeng, L., Wang, Z., Du, M., Wei, Q., Wang, Z., Wang, D., Zhen, Z., 2016. Spatial

and seasonal changes of arsenic species in Lake Taihu in relation to eutrophication. Sci. Total Environ. 563-564, 496-505.

Zamyadi, A., Choo, F., Newcombe, G., Stuetz, R., Henderson, R.K., 2016. A review of monitoring technologies for real-time management of cyanobacteria: recent advances and future direction. TRAC 85, S0165993615300406.

Zeng, P., Guo, Z., Xiao, X., Peng, C., 2019. Effects of tree-herb co-planting on the bacterial community composition and the relationship between specific microorganisms and enzymatic activities in metal(loid)-contaminated soil. Chemosphere 220, 237-248.

Zhang, J. Liu, Z., Wang, S., Jiang, P., 2002. Characterization of a bioflocculant produced by the marine myxobacterium Nannocystis sp NU-2. Appl. Microbiol. Biotechnol. 59, 517-522.

Zhu, Y. G., Yoshinaga, M., Zhao, F. J., Rosen, B.P., 2014. Earth abides arsenic biotransformations. Ann. Rev. Earth Planet. Sci. 42, 443-467.

Supporting Information

Seasonal variations in arsenic mobility and bacteria diversity of Huangshui Creek, Shimen Realgar Mine, Hunan Province, China

Wenxu Li [a], Jing Liu [b], Karen A. Hudson-Edwards [c,*]

[a] The Key Laboratory of Solid Waste Treatment and Resource Recycle, Ministry of Education, Southwest University of Science and Technology, Mianyang 621010 China

[b] College of Resources and Environment, Southwest University, Chongqing 400716 China

[c] Environment & Sustainability Institute and Camborne School of Mines, University of Exeter, Penryn, Cornwall TR10 9DF, UK. Tel: +44(0)1326-259489.

Submitted to: *Science of the Total Environment*

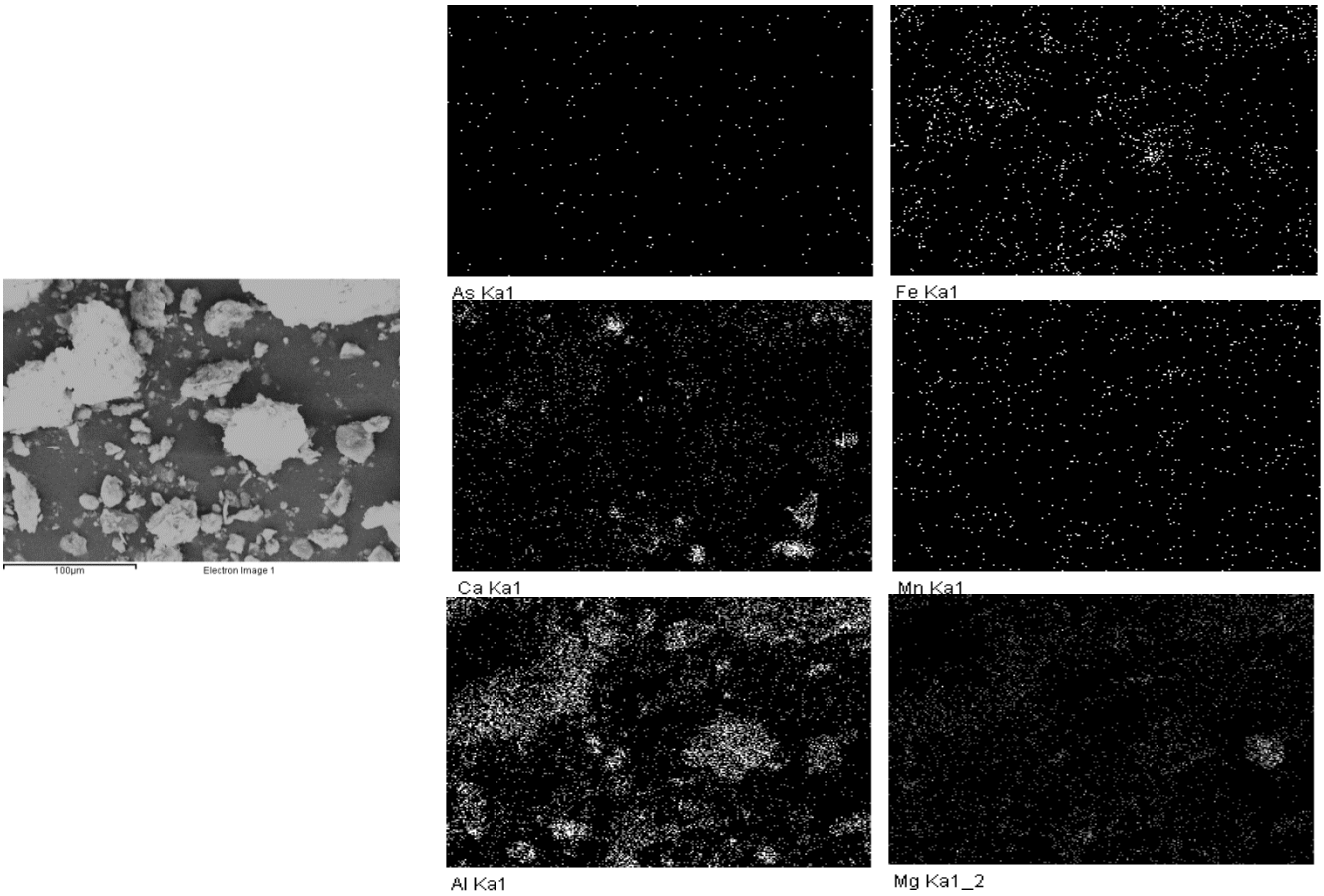

Figure S1. SEM-EDS elemental scans of sediment sample As9.

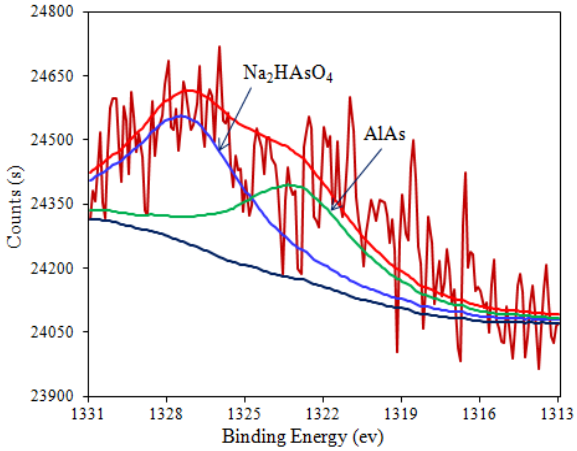

Fig S2. As (2p) XPS spectra of sediment sample As9.

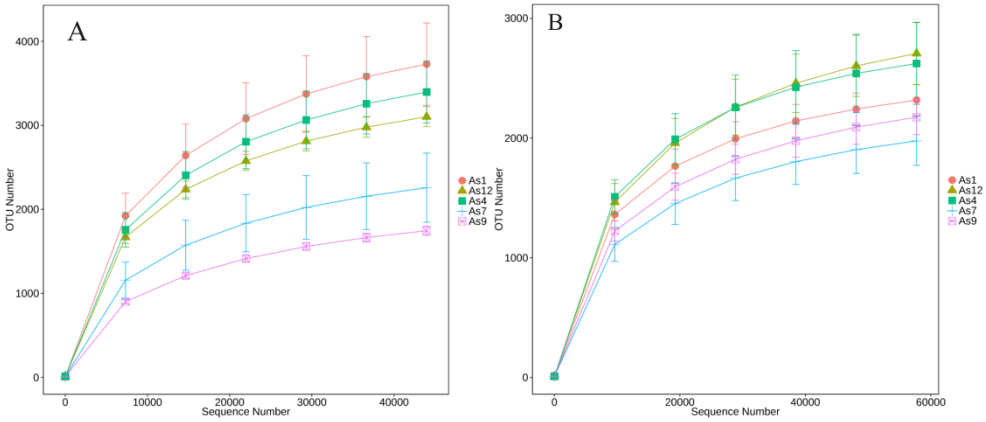

Fig. S3. Rarefaction curves for dry (A) and wet (B) season bacteria.

Table S1. Methods of microbial quenching and analysis.

Sequencing	
1.Extraction of genome DNA	Total genome DNA from samples was extracted using CTAB/SDS method. DNA concentration and purity was monitored on 1% agarose gels. According to the concentration, DNA was diluted to 1ng/μL using sterile water
2.Amplicon Generation	16S rRNA/18S rRNA/ITS genes of distinct regions (16S V4/16S V3/16S V3-V4/16S V4-V5, 18S V4/18S V9, ITS1/ITS2, Arc V4) were amplified used specific primer (e.g.16S V4: 515F-806R, 18S V4: 528F-706R, 18S V9: 1380F-1510R, et. al) with the barcode. All PCR reactions were carried out with Phusion® High-Fidelity PCR Master Mix (New England Biolabs).
3.PCR Products Mixing and Purification	Mix same volume of 1X loading buffer (contained SYB green) with PCR products and operate electrophoresis on 2% agarose gel for detection. PCR products was mixed in equidensity ratios. Then, mixture PCR products was purified with GeneJETTM Gel Extraction Kit (Thermo Scientific).
4.Library preparation and sequencing	Sequencing libraries were generated using Ion Plus Fragment Library Kit 48 rxns (Thermo Scientific) following manufacturer's recommendations. The library quality was assessed on the Qubit@ 2.0 Fluorometer (Thermo Scientific). At last, the library was sequenced on an Ion S5TM XL platform and 400 bp/600 bp single-end reads were generated.
Data analysis	
1.Single-end reads assembly and quality control	1.1 Data split Single-end reads was assigned to samples based on their unique barcode and truncated by cutting off the barcode and primer sequence. 1.2 Data Filtration Quality filtering on the raw reads were performed under specific filtering conditions to obtain the high-quality clean reads according to the Cutadapt (Martin, 2011) (V1.9.1, http://cutadapt.readthedocs.io/en/stable/)quality controlled process. 1.3 Chimera removal The reads were compared with the reference database (Gold database, http://drive5.com/uchime/uchime_download.html) using UCHIME algorithm (UCHIME Algorithm, http://www.drive5.com/usearch/manual/uchime_algo.html) (Edgar et al., 2011) to detect chimera sequences, and then the chimera sequences were removed (Haas et al., 2011). Then the Effective Tags finally obtained.
2. OTU cluster and Species annotation	2.1 OTU Production Sequences analysis were performed by Uparse software (Uparse v7.0.1001, http://drive5.com/uparse/) (Edgar 2013) . Sequences with ≥97% similarity were assigned to the same OTUs. Representative sequence for each OTU was screened for furtherannotation. 2.2 Species annotation For each representative sequence, the Silva Database (https://www.arb-silva.de/) (Quast et al., 2012) was used based on RDP classifier (Version 2.2, http://sourceforge.net/projects/rdp-classifier/) (Wang et al., 2007) algorithmto annotate taxonomic information. 2.3 Phylogenetic relationship Construction In order to study phylogenetic relationship of different OTUs, and the difference of the

	dominant species in different samples(groups), multiple sequence alignment wereconducted using the USCLE software (Version 3.8.31, http://www.drive5.com/muscle/) (Edgar 2004). 2.4 Data Normalization OTUs abundance information were normalized using a standard of sequence number corresponding to the sample with the least sequences. Subsequent analysis of alpha diversity and beta diversity were all performed basing on this output normalized data.
3. Alpha Diversity	Alpha diversity is applied in analyzing complexity of species diversity for a sample through6 indices, including Observed-species, Chao1, Shannon, Simpson, ACE, Good-coverage. All this indices in our samples were calculated with QIIME (Version1.7.0) and displayed with R software (Version 2.15.3). Two indices were selected to identify Community richness: Chao - the Chao1 estimator (http://www.mothur.org/wiki/Chao); ACE - the ACE estimator (http://www.mothur.org/wiki/Ace); Two indices were used to identify Community diversity: Shannon - the Shannon index (http://www.mothur.org/wiki/Shannon); Simpson - the Simpson index (http://www.mothur.org/wiki/Simpson); One indice to characterized Sequencing depth: Coverage - the Good's coverage (http://www.mothur.org/wiki/Coverage)
4. Beta Diversity	Beta diversity analysis was used to evaluate differences of samples in species complexity, Beta diversity on both weighted and unweighted unifrac were calculated by QIIME software (Version 1.7.0). Cluster analysis was preceded by principal component analysis (PCA), which was applied to reduce the dimension of the original variables using the FactoMineR package and ggplot2 package in R software (Version 2.15.3). Principal Coordinate Analysis (PCoA) was performed to get principal coordinates and visualize from complex, multidimensional data. A distance matrix of weighted or unweighted unifrac among samples obtained before was transformed to a new set of orthogonal axes, by which the maximum variation factor is demonstrated by first principal coordinate, and the second maximum one by the second principal coordinate, and so on. PCoA analysis was displayed by WGCNA package, stat packages and ggplot2 package in R software (Version 2.15.3). Unweighted Pair-group Method with Arithmetic Means (UPGMA) Clustering was performed as a type of hierarchical clustering method to interpret the distance matrix using average linkage and was conducted by QIIME software (Version 1.7.0).

Table S2. pH, Eh and T of dry and wet season water samples.

	Dry season				Wet season			
Samples	Q_H m^3/s	pH	Eh（mv）	T（℃）	Q_H m^3/s	pH	Eh（mv）	T（℃）
As1	0.022	8.12	-55.8	8.8	0.024	8.66	-89.53	26.1
As	0.02	8	-60.27	8.8	0.02	9.	-109.85	27.6

s2	2	.20			4	01		
As3	0.023	8.25	-62.87	8.8	0.038	9.2	-120.9	29.4
As4	0.002	7.45	-19.53	12.2	0.001	7.66	-33.15	21.7
As5	0.023	8.37	-69.2	8.8	0.039	9.21	-121.45	30.4
As6	/	7.57	-25.93	12.6	/	7.16	-12.8	23.5
As7	0.025	8.54	-78.83	9.0	0.058	10.21	-181.67	35.8
As8	/	8.04	-51.05	8.9	0.058	10.61	-204.1	35.6
As9	0.035	8.08	-53.8	9.3	0.059	10.58	-201.55	34.5
As10	/	8.11	-54.9	9.3	/	10.34	-188.4	34.6
As11	/	7.62	-28.4	12.6	/	7.5	-26	29.4
As12	0.035	8.15	-57.2	9.8	0.068	10.18	-178.9	34.3

Table S3. Major ATR-FTIR vibrations for As and S in sediments.

Vibration (cm-1)	Species	Assignment	Ref.
1003,1004	SO_4^{2-}	*v3*	(Usher et al., 2004, Roonasi and Holmgren 2009)
796,772	AsO_3^{3-}	*v1*	(Goldberg and Johnston 2001, Liu et al., 2013)
872	AsO_4^{3-}	*v3*	(Liu et al., 2017).
463	AsO_4^{3-}	*v4*	(Liu et al., 2017).
910	AsO_4^{3-}	As–O	(Goldberg and Johnston 2001)

Table S4. XRF data for dry season sediment samples.

Major oxides	Concentration (wt. %)				
	As1	As4	As7	As9	As12
SiO_2	64.88	70.61	56.83	52.27	64.50
Al_2O_3	16.26	15.14	17.36	16.12	17.56
CaO	6.45	2.60	9.67	17.10	4.32
Fe_2O_3	5.67	5.30	6.82	6.42	6.37
K_2O	3.07	2.94	3.79	2.85	3.38
MgO	1.66	1.44	2.07	1.79	1.75
TiO_2	0.77	0.69	0.84	0.85	0.72
P_2O_5	0.36	0.29	1.05	1.00	0.29
Others	0.87	0.92	1.43	1.45	1.04

Table S5. Arsenic concentrations in dry and wet season sediment samples

sites	Dry season (μg g^{-1})	Wet season (μg g^{-1})
As1	120	103
As4	590	521
As7	964	1310
As9	992	1700
As12	564	675

References

Edgar, R.C., 2004. Muscle: multiple sequence alignment with high accuracy and high throughput. Nucleic Acids Res. 32, 1792-1797.

Edgar, R.C., 2013. Uparse: highly accurate OTU sequences from microbial amplicon reads. Nat. Methods 10, 996-998.

Edgar, R.C., Haas, B.J., Clemente, J. ., Quince, C., Knight, R., 2011. Uchime improves sensitivity and speed of chimera detection. Bioinformatics 27, 2194-2200.

Goldberg, S., Johnston, C.T., 2001. Mechanisms of arsenic sdsorption on smorphous oxides rvaluated using macroscopic measurements, vibrational spectroscopy, and surface complexation modeling. J. Colloid Interf. Sci. 234, 204-216.

Haas, B.J., Gevers, D., Earl, A.M., Feldgarden, M., Ward, D.V., Giannoukos, G., Ciulla, D., Tabbaa, D., Highlander, S.K., Sodergren, E., 2011. Chimeric 16S rRNA sequence formation and detection in Sanger and 454-pyrosequenced PCR amplicons. Genome Res 21(3), 494-504.

Liu, J., Cheng, H., Frost, R.L., Dong, F., 2013. The mineral tooeleite $Fe_6(AsO_3)_4SO_4(OH)_4{\cdot}4H_2O$ – An infrared and Raman spectroscopic study-environmental implications for arsenic remediation. Spectrochim. Acta A Mol. Biomol. Spectrosc. 103, 272-275.

Liu, J., He, L., Dong, F. Q., Frost, R. L., 2017. Infrared and Raman spectroscopic characterizations on new Fe sulphoarsenate hilarionite ($Fe_2((III))(SO_4)(AsO_4)(OH)\cdot 6H_2O$): Implications for arsenic mineralogy in supergene environment of mine area. Spectrochim. Acta Pt A Mol Biomol Spectrosc. 170, 9-13.

Martin, M., 2011. Cutadapt removes adapter sequences from high-throughput sequencing reads. EMBnet.journal 17, 10-12.

Matschullat, J., 2000. Arsenic in the geosphere—a review. Sci. Total Environ. 249, 297-312.

Quast, C., Pruesse, E., Yilmaz, P., Gerken, J., Schweer, T., Yarza, P., Peplies, J. 2012. The Silva ribosomal RNA gene database project: improved data processing and web-based tools. Nucleic Acids Res 41, D590-D596.

Roonasi, P., Holmgren, A., 2009. An ATR-FTIR study of sulphate sorption on magnetite; rate of adsorption, surface speciation, and effect of calcium ions. J. Colloid Interf. Sci. 333, 27-32.

Usher, C.R., Cleveland, C.A., Strongin, D.R., Schoonen, M.A., 2004. Origin of oxygen in sulfate during pyrite oxidation with water and dissolved oxygen: An in situ horizontal attenuated total reflectance infrared spectroscopy isotope study. Environ. Sci. Technol. 38, 5604-5606.

Wang, Q., Garrity, G.M., Tiedje, J.M., Cole, J.R., 2007. Naive Bayesian classifier for rapid assignment of rRNA sequences into the new bacterial taxonomy. Appl. Environ. Microbiol. 73, 5261-5267.